

Palaeogenomic analysis of black rat (*Rattus rattus*) reveals multiple European introductions associated with human economic history

He Yu^{1,2,3,61}, Alexandra Jamieson^{4,61}, Ardern Hulme-Beaman^{5,6}, Chris J. Conroy ⁷, Becky Knight⁸, Camilla Speller^{9,10}, Hiba Al-Jarah⁹, Heidi Eager¹¹, Alexandra Trinks^{4,12}, Gamini Adikari¹³, Henriette Baron¹⁴, Beate Böhlendorf-Arslan¹⁵, Wijerathne Bohingamuwa ¹⁶, Alison Crowther^{17,18}, Thomas Cucchi¹⁹, Kinie Esser²⁰, Jeffrey Fleisher ²¹, Louisa Gidney²², Elena Gladilina²³, Pavel Gol'din ²⁴, Steven M. Goodman ²⁵, Sheila Hamilton-Dyer²⁶, Richard Helm ²⁷, Jesse C. Hillman²⁸, Nabil Kallala^{29,30}, Hanna Kivikero^{31,32}, Zsófia E. Kovács³³, Günther Karl Kunst³⁴, René Kysely ³⁵, Anna Linderholm ^{4,36}, Bouthéina Maraoui-Telmini³⁷, Nemanja Marković ³⁸, Arturo Morales-Muñiz³⁹, Mariana Nabais ^{40,41}, Terry O'Connor⁹, Tarek Oueslati ⁴², Eréndira M. Quintana Morales ⁴³, Kerstin Pasda ⁴⁴, Jude Perera⁴⁵, Nimal Perera⁴⁵, Silvia Radbauer⁴⁶, Joan Ramon⁴⁷, Eve Rannamäe ⁴⁸, Joan Sanmartí Grego⁴⁹, Edward Treasure⁵⁰, Silvia Valenzuela-Lamas ⁵¹, Inge van der Jagt⁵², Wim Van Neer ^{53,54}, Jean-Denis Vigne¹⁹, Thomas Walker⁵⁵, Stephanie Wynne-Jones ⁸, Jørn Zeiler⁵⁶, Keith Dobney ^{5,57,58,59}, Nicole Boivin ^{17,18}, Jeremy B. Searle ¹¹, Ben Krause-Kyora ⁶⁰, Johannes Krause ^{1,3✉}, Greger Larson ^{4✉} & David Orton ^{9✉}

The distribution of the black rat (*Rattus rattus*) has been heavily influenced by its association with humans. The dispersal history of this non-native commensal rodent across Europe, however, remains poorly understood, and different introductions may have occurred during the Roman and medieval periods. Here, in order to reconstruct the population history of European black rats, we first generate a de novo genome assembly of the black rat. We then sequence 67 ancient and three modern black rat mitogenomes, and 36 ancient and three modern nuclear genomes from archaeological sites spanning the 1st-17th centuries CE in Europe and North Africa. Analyses of our newly reported sequences, together with published mitochondrial DNA sequences, confirm that black rats were introduced into the Mediterranean and Europe from Southwest Asia. Genomic analyses of the ancient rats reveal a population turnover in temperate Europe between the 6th and 10th centuries CE, coincident with an archaeologically attested decline in the black rat population. The near disappearance and re-emergence of black rats in Europe may have been the result of the breakdown of the Roman Empire, the First Plague Pandemic, and/or post-Roman climatic cooling.

The black rat (*Rattus rattus*) is one of three rodent species, along with the house mouse (*Mus musculus*) and brown rat (*R. norvegicus*), to have become globally distributed thanks to a close commensal relationship with humans¹. Collectively, these taxa are highly significant to human societies both as pests responsible for billions of euros of damage to food stores annually², and as vectors and/or reservoirs that have contributed to the spread of numerous diseases, most famously bubonic plague^{3,4}.

Despite the significance of this rodent, our knowledge of the black rat's evolutionary history and taxonomy remains limited. Previous genetic studies have described a *R. rattus* complex involving multiple recognised species with potential introgression among different lineages^{5–7}. Mitochondrial DNA studies have helped to resolve the taxonomic controversies by linking a monophyletic mitochondrial lineage to specific South Asian (now globally distributed) black rat populations that possess a $2n = 38$ karyotype (previously referred to as lineage I)^{8–10}. The Asian house rat (*R. tanezumi*), endemic to Southeast Asia, has been identified as the closest sister group of the black rat (previously designated as lineages II through IV). The divergence between the two species has been dated to ~0.4 Mya¹¹, and the two have been suggested to hybridise^{6,7,12}.

The ability of rats to colonise, and become dependent upon anthropogenic niches¹³ makes them ideal bioproxies to track historical processes^{1,14,15}. Archaeological specimens of rats and mice have thus been used to track human migrations, trade, and settlement types in a wide range of contexts^{16–22}. Previous archaeological and genetic evidence suggests that the pre-commensal distribution of the Eurasian black rat (based on the taxonomic definition proposed by mitochondrial DNA studies^{8,9} and hereafter referred to as black rat, see SI for discussion) was largely limited to South Asia^{10,23,24}. Black rat finds from cave sediments in the Levant spanning the late Pleistocene to early Holocene indicate a possible western distribution^{25,26}. These remains, however, require direct dating to confirm their age, and there is a subsequent absence of rats from settlement sites in this region until at least the second millennium BCE²⁶.

The earliest large concentrations of presumed commensal rat remains reported thus far derive from late third, or early second millennium BCE settlements in both the Indus Valley and Mesopotamia²⁶. Commensal black rats may also have reached the Levant and eastern Mediterranean region by the start of the first millennium BCE²⁶. Based on archaeological evidence from Corsica, the Balearics, Italy and Morocco^{27–29}, black rats likely first appeared in the western Mediterranean basin towards the end of that same millennium.

The black rat's colonisation of Europe has been linked to the historical development of urbanism and trade networks, and their arrival is important for understanding historical plague pandemics including the 6th century Justinianic Plague and the 14th century Black Death^{4,30–32}. The central role traditionally attributed to black rats and their fleas in the spread of the plague bacterium (*Yersinia pestis*) during these pandemics has been challenged on various grounds, however, including the historical distribution and abundance of rats, and this correlation continues to be debated^{33–37}.

Although surveys of zooarchaeological rat finds from archaeological sites across Europe suffer from considerable regional variation in coverage, the available data indicates successive episodes of dispersal north of the Mediterranean associated first with Roman expansion (first century BCE to second century CE), and then with the emergence of medieval economies from the 9th century CE, punctuated by a decline and a possible range contraction³². Black rat remains are found throughout the Roman Empire in the 1st–5th centuries CE, but rarely beyond its

northern borders, suggesting that these rats were dependent on a Roman economic system characterised by a network of dense settlements connected by bulk transport via efficient road, river, and maritime routes^{4,31}.

With the breakdown of the Roman Empire from the 5th century onwards, evidence for the existence of black rats becomes scarcer. They may have been extirpated entirely from the northern provinces including Britain^{32,38,39}, and the percentage of archaeological sites with black rat remains declined even in the Western Empire's Italian core⁴⁰. By contrast, black rats remained common in the Balkans and Anatolia until at least the 6th century CE, presumably reflecting continued stability in the Eastern Roman Empire^{41–44}. Since zooarchaeological data between the 5th–8th centuries is limited in many European and Mediterranean regions, the pattern of post-Roman absence may partly represent research bias⁴⁵, though early medieval black rats are rare even where other small mammals are reported³⁸.

Black rats reappeared at northern European trading settlements during the 9th and 10th centuries CE, including sites well beyond their prior Roman range, including Hedeby in northern Germany and Birka in Sweden, as well as former Roman towns and high-status early medieval settlements such as York and Flixborough in England and Sulzbach in Bavaria^{46–50}. The subsequent expansion of urbanism and large-scale trade of bulk goods in medieval Europe appears to have favoured rats, just as in the Roman period. By the 13th century CE, black rats were present throughout most of Europe⁴ and they reached southern Finland by the late 14th century⁵¹. Black rats remained widespread across Europe until at least the 18th century, before their population declined, most likely as a result of competition with the newly arrived brown rat, the rat species that is now dominant in temperate Europe^{52–54}.

It remains unclear whether the black rat was actually extirpated from post-Roman northern and western Europe; and whether medieval rat populations in temperate Europe derived from the remnant population in southern Europe, or from another wave of rats that were introduced from beyond the Mediterranean (e.g. via Rus' river trade^{32,55}). These questions are relevant to several key debates in European economic and environmental history including: (1) the extent to which the end of the Western Roman Empire represented a crisis in urbanism and trade—particularly in bulk goods such as grain—as well as a political collapse^{56–58}; (2) the role of easterly vs. westerly connections in the rise of northern European medieval urban networks^{59,60}; and (3) the model of the spread of the Justinianic Plague and the subsequent First Pandemic. This pandemic started in the eastern Mediterranean in 541 CE, spread quickly across Europe including England, and continued for approximately two centuries^{61–63}, a period that coincides with the gap in archaeological evidence for rats in northwest Europe. Given the limitations of both zooarchaeology and genetic studies of modern rat populations to address successive waves of contact after a species is established, ancient DNA may help to resolve these questions by directly revealing the presence or lack of genetic continuity through time.

Here, we employ a nested three-stage approach to address these questions. First, we assemble a de novo reference genome of the black rat. This genome allows us to investigate the long-term demographic history of the black rat in relation to other rat species, and to establish the foundation for genome-wide analyses of ancient remains. Second, we report 70 new mitochondrial genomes from 3 modern and 67 ancient European and North African black rats, including archaeological specimens spanning the Roman to early post-medieval periods (1st–17th century CE). We explore the dispersal of black rats into the Mediterranean and Europe by analysing these alongside 132 mitochondrial DNA sequences (106 historic and 26 modern) generated from modern

Table 1 Assembly statistics of the de novo black rat reference genome.

Scaffold number	6805
Scaffold N50 (Mb)	145.8
Largest scaffold (Mb)	260.8
Assembly size (Gb)	2.25
Scaffold length >10 Mb (Gb)	2.23
GC content (%)	42.1
Repetitive region (%)	38.4

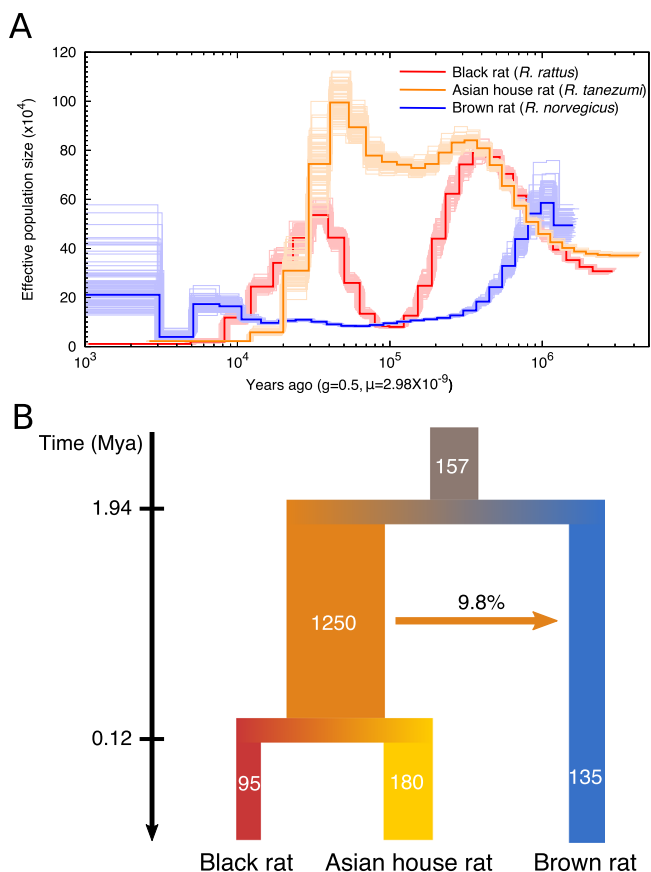


Fig. 1 The demographic history of the black rat and its closely related species. **A** Population dynamics of the black rat (*R. rattus*), Asian house rat (*R. tanezumi*) and brown rat (*R. norvegicus*) estimated by PSMC, with 100 bootstrap replicates. **B** Demographic modelling of the divergence and migration among the black rat, Asian house rat and brown rat estimated by G-PhoCS. The values represent the average estimates of effective population sizes (in thousands), population divergence times (Mya) and the total migration rate through time. The 95% HPD range of all estimates are listed in Supplementary Data 1.

and museum black rat specimens from across western Eurasia, the Indian Ocean, and Africa. Lastly, we generate 36 nuclear genomes from our archaeological black rats and three from modern black rats and use these to explore the species’ population history in Europe and the Mediterranean from the 1st to 17th centuries CE, focusing particularly on the hypothesis of dual dispersals in the Roman and medieval periods. We then interpret the black rat’s dispersal history within the context of major historical processes.

Results

The demographic history of the black rat and its closely related species. To facilitate the study of the demographic history of the black rat, both before and after the establishment of its commensal relationship with humans, we first generated a de novo genome assembly of the black rat using a wild-caught individual from California, USA (Supplementary Note 1). Combining shotgun, Chicago and Hi-C sequencing data with the Dovetail HiRise assembler pipeline⁶⁴, we obtained a genome assembly with a total length of 2.25 Gb and a scaffold N50 reaching 145.8 Mb (Supplementary Tables 1 and 2). The 22 scaffolds with over 10 Mb covering 98.9% of the entire assembly (Table 1), with each of the 18 autosomes corresponding to one large scaffold each and over 90% of the X chromosome represented by four scaffolds (Supplementary Figs. 1 and 2, Supplementary Note 1). The average GC content is 42.1%, similar to the brown rat reference genome *Rnor_6.0* (42.3%), and 38.4% of the assembly was identified as repetitive elements (Supplementary Table 3). Benchmarking Universal Single-Copy Orthologs (BUSCO) analysis⁶⁵ also revealed a high completeness of this genome assembly, with 90.1% complete BUSCOs identified using eukaryotic dataset, comparable with *Rnor_6.0* (91.4%) (Supplementary Table 4). Because the Asian house rat and the black rat are both present in California, we also assessed potential introgression from the Asian house rat into our black rat individual. A signature of introgression would limit the value of our de novo genome as a reference genome onto which reads derived from ancient black rats could be mapped. Our analyses suggested no significant introgression signature in the Californian black rat (Supplementary Note 1, Supplementary Table 5).

To address the demographic history of black rat, we applied the pairwise sequentially Markovian coalescent (PSMC)⁶⁶ analysis to estimate its population size dynamics alongside the brown rat and Asian house rat. When calibrated with a mutation rate of 2.96×10^{-9} per generation and generation time of 0.5 years⁶⁷, the analyses revealed different dynamic patterns of population size changes amongst these rat species (Fig. 1A). The brown rat experienced a population decline beginning ~1 Mya, as described previously⁶⁷, while both the black rat and Asian house rat populations expanded until 300–400 thousand years ago (kya). The black rat population then experienced a bottleneck with an 8-fold drop in effective population size until 100 kya, and a re-expansion from 100 to 40 kya. The Asian house rat, however, did not experience a population decline until ~40 kya, when both black rat and Asian house rat populations experienced declines that have continued to the present.

To investigate the population sizes, split times, and migrations among these rat lineages, we applied Generalised Phylogenetic Coalescent Sampler (G-PhoCS)⁶⁸. The result revealed a similar population size dynamism, with the effective population size (N_e) of black rat/Asian house rat ancestral lineage estimated to be 1.25×10^6 , about tenfold the N_e of black rat/Asian house rat/brown rat lineages (Fig. 1B, Supplementary Note 2, Supplementary Data 1). The split time between brown rat and black rat/Asian house rat lineages was estimated to be 1.94 Mya (within the 95% highest posterior density (HPD) range estimated using mitochondrial genomes in a previous study¹¹), while the split of Asian house rat and black rat lineages took place ~120 kya. This recent split time relative to the coalescent time estimate based on mitochondrial genomes between these two lineages could be explained by the large ancestral population size of the black rat/Asian house rat lineage⁶⁸. Among these lineages, we only detected one instance of gene flow from the black rat/Asian house rat ancestral lineage into brown rat lineage, with an introgression proportion of 9.8%.

Taken together, we observed population expansions and bottlenecks in the black rat during the last million years, and a smaller N_e relative to the Asian house rat. This could be explained by the relatively limited geographic distribution of the black rat in southern Asia before the initiation of its commensal relationship with people, and the fact that the Asian house rat is endemic to a much greater area in southeastern Asia¹⁰. We did not detect any genomic introgression between the lineages leading to the black and Asian house rat, suggesting these two species were geographically isolated after their split from a common ancestor for a sufficiently long period to facilitate their reproductive incompatibility.

A global phylogeography of the black rat based on mitochondrial DNA. We collected 191 ancient black rat individuals from 33 archaeological sites across Europe, North and East Africa, and southern Asia dating from the 2nd millennium BCE to the 17th century CE, plus eight modern individuals from North Africa (Supplementary Note 3, Supplementary Data 2). After shotgun screening, we retrieved 70 mitochondrial genomes (67 ancient and 3 modern, with coverage spanning 3.5×–300.0×) from samples from 18 sites in Europe and the Mediterranean (Supplementary Data 2), and identified 40 haplotypes. The phylogenetic tree based on mitochondrial genomes revealed two clades: a major clade with 32 haplotypes from 47 ancient and modern samples, together with the modern Californian rat, and a minor clade consisting of eight haplotypes and 23 ancient samples from the 6th-century site of Caričin Grad, Serbia (Supplementary Fig. 3). The phylogenetic resolution within each major clade was relatively poor, though samples from the same or closely related

sites occasionally formed sub-clades including the samples from modern-day Zembra (Tunisia) and medieval central Europe.

In order to establish the relationship between the ancient rats and modern black rats from across their range, we analysed the cytochrome b (CYTB) region from 476 samples, including our 67 ancient samples and three modern samples alongside 132 previously unpublished modern and historic CYTB sequences from across the Indian Ocean basin (Supplementary Data 2), and 274 sequences published in previous studies^{10,24,69,70}. The maximum-likelihood tree of the CYTB region revealed that all the ancient rats from this study belong to the previously described black rat lineage I (Fig. 2, Supplementary Figs. 4, 5 and Supplementary Data 2). None of the ancient rats from this study fell into *Rattus* lineages II–VI. Within lineage I, we recapitulated the unnamed substructure and assigned the terms A–E to the five major haplogroups¹⁰. In addition to these five, we confirmed a sixth lineage I haplogroup, F, consisting of modern samples from Sri Lanka and the Andaman Islands, which is basal relative to all other lineage I black rats and has previously been reported as the Sri Lankan unique sub-lineage, RrC LIB⁷¹ (Fig. 2, Supplementary Fig. 4B, Supplementary Data 2).

Haplogroup A within lineage I (previously described as the European ship rat²⁴) was the most common among the analysed samples (179/354). Members of this haplogroup include ancient and modern black rats from Europe and regions of the world with a history of colonisation by, and/or trade with European powers. The only additional haplogroup found in Europe was Haplogroup C (previously described as the Arab ship rat²⁴) at Caričin Grad, Serbia, which included 24 archaeological individuals. Haplogroup C is found in modern rats from India, Egypt, East, South and

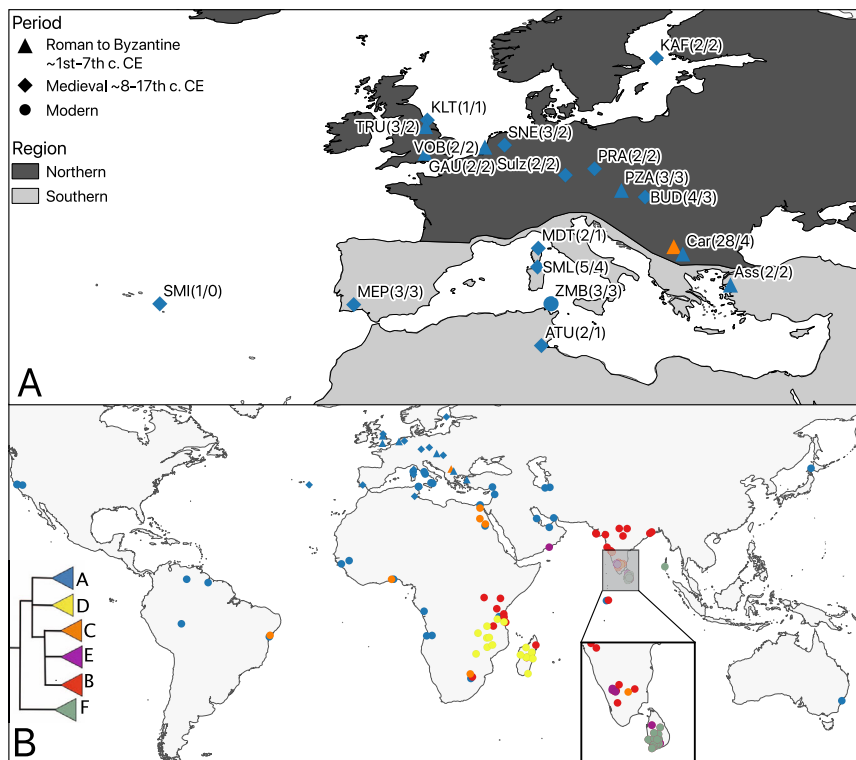


Fig. 2 Sampling sites and mitochondrial phylogeographic patterns. **A** Map of sampling locations. The numbers in parentheses are numbers of samples included in mitochondrial/nuclear genome analysis. SMI (Villa Franca do Campo), MEP (Mertola), KLT (Kilton Castle), TRU (Tanner Row, York), GAU (Gatehampton Villa), VOB (Voorburg-Forum Hadriani), SNE (Deventer-Stadhuiskwartier), MDT (Monte di Tuda), SML (Santa Maria Lavezzi), ATU (Althiburos), Sulz (Castle Sulzbach), PRA (Prague Castle), PZA (Petronell-Carnuntum Zivilstadt), KAF (Kastelholm), BUD (Buda Castle-Teleki Palace), Car (Caričin Grad) and Ass (Assos). **B** The phylogeographic pattern of black rat revealed by CYTB mitochondrial haplogroups (see Supplementary Fig. 4 for detailed phylogeny), including 67 ancient rats, 3 modern rats from Zembra, 132 modern samples from Indian Ocean basin and 274 published samples. Basemap source: ESRI ArcWorld Supplement (World Continents), used under license.

West Africa, and South America. None of the other haplogroups were present in Europe or the Mediterranean region. Haplogroups B and E only included modern samples from India and countries bordering the Indian Ocean. Haplogroup D (previously described as the Madagascar and Indian Ocean islands group²⁴) included primarily samples from Madagascar and East Africa, and Haplogroup F consisted of samples from Sri Lanka and the Andaman Islands (Fig. 2, Supplementary Data 2).

To investigate the introduction route of black rats into Europe, we analysed mitochondrial cytochrome B sequences derived from globally distributed modern and ancient black rats. Previous studies indicated that the black rat originated in the Indian Peninsula^{10,24,69,72}. Leaving aside the putative Late Pleistocene to early Holocene records from the eastern Levant, the earliest finds of presumed commensal black rats derive from the Indus Valley and Mesopotamia in the 3rd/2nd millennium BCE, coincident with the emergence of urbanism and establishment of trade links between these regions^{26,73}, though a more westerly limit to the black rat's natal range cannot be excluded. The source for dispersal to the Mediterranean and ultimately Europe remains unclear. Suggestions include maritime trade from India and/or the Arabian peninsula into the Red Sea and subsequently through Egypt (perhaps via the canal built under Darius⁷⁴) in the mid/late first millennium BCE^{4,32}, or more likely earlier overland communication routes between Mesopotamia and the Levant^{26,73}.

While a maritime route is clearly implicated in the black rat's dispersal to East Africa^{75,76}, our results tentatively favour an overland hypothesis for its dispersal from South Asia to the Mediterranean to Europe, since both ancient and modern black rats from Europe and the eastern Mediterranean share haplogroups with sampled populations from Iran and the Persian Gulf, but not with Indian Ocean samples from southern India to Madagascar (Fig. 2). The results also suggest a secondary dispersal route via Egypt, given the appearance of Haplogroup C at the 6th century CE Byzantine site of Caričin Grad, Serbia and in modern samples from the Nile valley. While hypothetical, this might reflect Egypt's central roles both in direct Indo-Roman trade, following its annexation in 30 BCE, and in grain production for the Roman and early Byzantine Empires^{4,77}. To test these hypotheses, further investigations into ancient and modern black rat populations from the Levant, Mesopotamia, Egypt and the Indus Valley are necessary.

Ancient genomes reveal the relationships of European black rats over space and time. To explore the black rat's European population history in greater detail, we shotgun sequenced 36 ancient and three modern black rats from 17 sites to 0.2×–16× coverage for whole genome analysis, including 18 females and 21 males determined by the coverage on sex chromosomes (Supplementary Data 2). The deeper sequenced ancient samples spanned two broad time periods, including 15 from the Roman and Early Byzantine period (1st–7th century CE), and 21 from medieval and post-medieval contexts (8th–17th century CE) (Supplementary Data 3). Geographically, all the samples were divided into two groups: a “northern” group of 25 samples from temperate Europe, and a “southern” group of 11 samples from the Mediterranean and Portugal (Fig. 2). After mapping and genotyping, we identified 7,869,069 bi-allelic transversion variants in the autosomal non-repetitive regions. They were combined with the Californian black rat for de novo genome assembly, and two published brown rats and one published Asian house rat for downstream population genomic analyses.

The phylogenetic tree constructed from autosomal SNPs revealed complex relationships among ancient black rats from different regions and time periods (Fig. 3A). Except for the late

medieval (ca. 14th century) to Ottoman (ca. 17th century) site of Buda Castle, Hungary, samples from the same site are clustered together. All the samples from the northern group, together with one southern sample from the medieval period—from 8th to 9th century Althiburos, Tunisia—formed a single clade, while all the other Byzantine to medieval samples from the southern group formed several separate clades consistent with their local geographic region. The rats from the southern group also possessed higher heterozygosity than those from the northern group, within both Roman/Byzantine and medieval/post-medieval periods (Supplementary Fig. 6, Supplementary Table 7, Supplementary Data 4). This could be explained by the longer history of rats in the Mediterranean which date to at least the first millennium BCE^{26,27}, and the founder effects of limited introductory waves of rats into the northern region.

Within the major northern cluster, samples were divided into two smaller clusters representing Roman/Byzantine and medieval/post-medieval periods, respectively. The only exception was a medieval Tunisian sample that falls into the Roman cluster. Within each cluster, samples grouped together based upon their geographic location (central Europe, western/northern Europe, Serbia). These phylogenetic relationships suggest that the initial black rat population in temperate Europe was replaced by a genetically distinct population after the 6th century CE. The younger population was first documented in early medieval (8th to early 10th century CE) Sulzbach, Germany. The Roman-like gene pool was still present during the 8th–9th century in North Africa, though due to the lack of more recent samples we cannot address whether or when the second wave arrived there. A similar pattern was also revealed by multidimensional scaling (MDS) based on isolation-by-state (IBS) distance among the samples (Supplementary Fig. 7).

The phylogenetic tree based on Y-chromosome scpMSY regions (Supplementary Data 5) similarly demonstrated that the Roman rats formed a single cluster. However, unlike the autosomal phylogeny, all the post-Roman samples from both the northern and southern groups, including Byzantine Assos and Caričin grad, formed a separate cluster (Supplementary Fig. 8), without well-supported substructures. Given the male-biased dispersal pattern commonly described in the black rat and other rodent species^{78,79}, this might indicate a male-specific replacement that took place in both the Mediterranean regions and temperate Europe.

A decline in the European black rat population during the 6th–9th centuries has previously been suggested based on zooarchaeological evidence^{32,38,39}. This has been attributed to several causes including: (a) the demise of the Western Roman Empire's economic and urban system from the 5th century CE, including the cessation of large-scale grain shipments that may have helped to disperse and support rat populations⁴; (b) climatic cooling in the ‘Late Antique Little Ice Age’⁸⁰; and/or (c) the Justinianic Plague, which began in 541 CE and is likely to have infected rat populations previously naive to *Yersinia pestis*, regardless of their potential role in its spread among humans^{4,81,82}. Our finding of a post-6th-century turnover corroborates this apparent decline, though the density of our samples' spatiotemporal coverage is not sufficient for us to distinguish between the potential causes. To understand how the Justinianic Plague influenced the rat population, further studies should focus on archaeological black rats from contexts post-dating the mid-6th century in areas of the Byzantine Empire and wider Mediterranean where an urban settlement system persisted.

The medieval Tunisian (Althiburos) sample indicates a different population history of black rats in North Africa relative to temperate Europe. Black rats from a wider range of time periods resident in North Africa and the western Mediterranean would allow us to test whether there was continuity within the

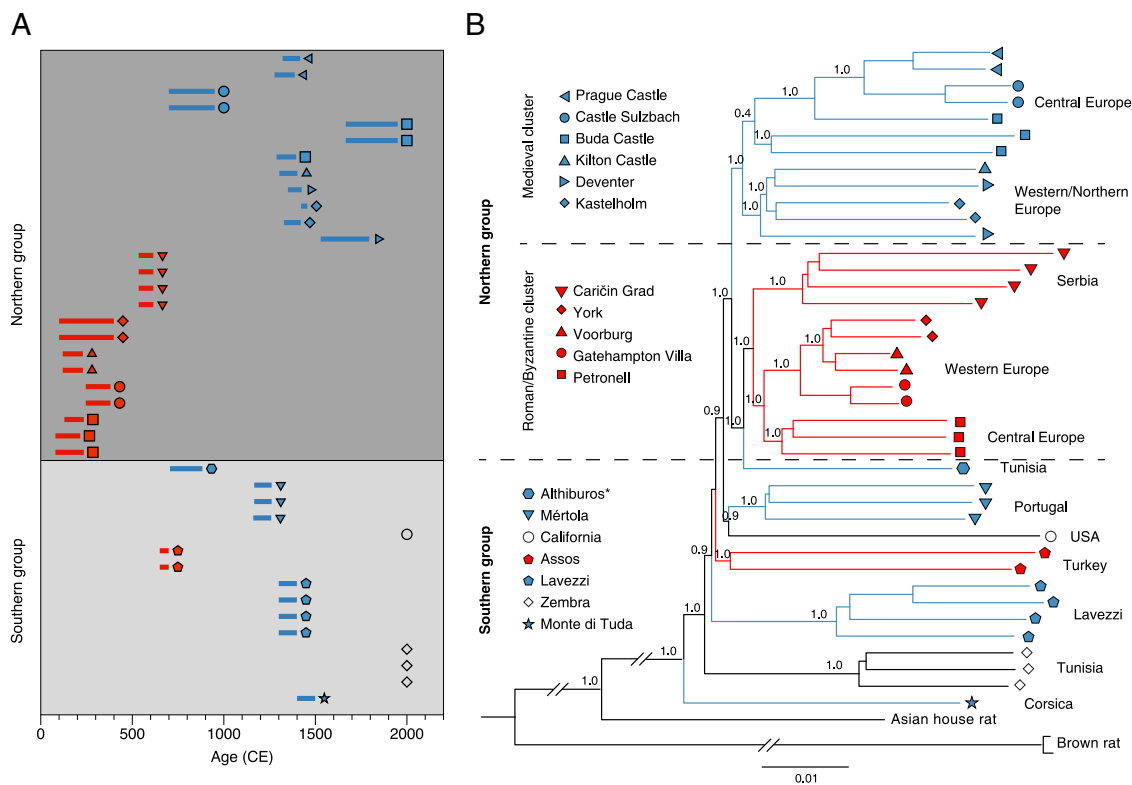


Fig. 3 Relationships of the ancient black rats over time and space. A The ages of the rat samples included in whole genome analyses. The bars represent 95.4% confidence intervals surrounding the direct radiocarbon dates or stratigraphic dates (Supplementary Data 3). The colours correspond to the Roman/Byzantine (red) and medieval (blue) time periods. The symbols represent the sampling sites listed in panel B, and the modern samples are represented by black symbols. **B** The phylogenetic relationship among ancient and modern black rats reconstructed using a neighbour joining phylogeny. The pairwise genetic distances were calculated using autosomal variants. The support values based upon 100 bootstrap replicates are shown on the nodes. The branches are coloured by sample ages as described in panel A, and the tip symbols correspond to the sampling site. * Though the medieval Tunisian (Althiburos) sample clusters geographically in the southern group, it falls in with the Roman cluster of the northern group in the phylogeny.

black rat populations from the Roman to early Islamic period (ca. 8th century). This is particularly pertinent to debates concerning the degree of continuity between the Roman Empire and the Early Islamic world, notably in urban settlements and trade networks⁸³.

To investigate the genetic interaction between different rat populations further, we applied a series of f -statistics. Based on the result of the f_4 -statistics symmetry test, the ancient samples were divided into 18 groups (Supplementary Data 4). Of these, 16 correspond to samples from 16 different sites, while the three late/post-medieval samples from Buda Castle (Hungary) fell into two groups corresponding, respectively, to late medieval (14th–15th century) and Ottoman (17th century) periods (Supplementary Data 3).

First, we investigated if any Roman population contributed to the Byzantine or medieval groups, with f_4 (norvegicus, Byzantine/medieval; Roman1, Roman2). We found that of two Roman geographical groups (central European represented by Austria, and western Europe represented by Britain and the Netherlands) the western rats were significantly more closely related to all the Byzantine and medieval groups (Fig. 4A, Supplementary Fig. 9, Supplementary Data 4). This result suggests that despite the population turnover that occurred in temperate Europe after the Roman period, Roman black rats from western Europe may have contributed to populations that colonised temperate Europe following the decline of the original population.

Next, we applied f_4 (norvegicus, Roman; Byzantine/medieval1, Byzantine/medieval2) to test if there were any differences in the relative contribution of Roman rat ancestry into the Byzantine or

medieval populations. In agreement with the phylogenetic and MDS analysis, most northern groups were significantly more closely related to the Roman rat populations compared to the Byzantine or more recent southern groups (SML, MDT, Ass). The lone exception to this pattern were two post-medieval samples from Buda Castle (BUD001/4), which were equally related to the Roman groups and the Assos (Ass) group that consists of two samples from Byzantine Turkey (Supplementary Data 4). Among the northern groups, the medieval rats from Åland (Finland), the UK, and the Netherlands, as well as Byzantine rats from Serbia, were more closely related to the Roman rat populations than were medieval rats from central Europe (represented by populations in Germany, Czech Republic, and Hungary). This suggests that the genetic contribution from putatively western European Roman rats, was also greater in the local western European medieval rats.

We also investigated the relationship between the Buda Castle (Hungary) samples from different time periods by contrasting them with the other medieval rats from temperate Europe (Fig. 4A, Supplementary Fig. 9, Supplementary Data 4). As revealed by the phylogenetic tree, both the German and Czech rats shared more genetic affinity with the ca. 14th–15th century Buda Castle (BUD003) sample, than with the 17th century or later specimens (BUD001/4). Having said that, BUD001/4 still showed higher affinity to BUD003, when compared with all other populations. This evidence suggests a black rat population transition in this region between the 14th/15th century and the late 17th century, potentially related to the 16th–17th century Ottoman occupation of Buda (Hungary), while the local medieval ancestry was still present in the later population.

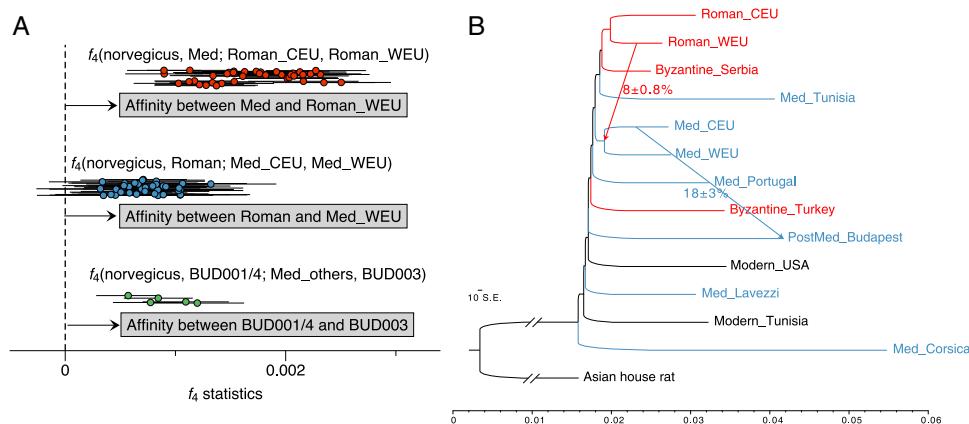


Fig. 4 Gene flow among ancient rat populations. **A** The f_4 -statistics showing admixture between different ancient rat populations. The dots show all the combinations of f_4 -statistics as described above each cluster, with the center being f_4 values and the error bars being $\pm 3SE$ of the estimates. The SE is determined using jackknife with sample size (n) being the number of autosomal scaffolds. The three clusters show the affinity between: (top, red) medieval rats (Med) and western European Roman rats (Roman_WEU); (middle, blue) Roman rats (Roman) and western European medieval rats (Med_WEU); and (bottom, green) post-medieval Buda Castle rats (BUD001/4) and the medieval Buda Castle rat (BUD003), respectively. The source data is provided in Supplementary Data 4.2, 4.3 and 4.4. **B** Admixture graph with two migration events fitted, estimated by Treemix. The migration edges are displayed by arrow including the introgression fractions and standard errors. The colour of each branch represents the time period of each group: Roman/Byzantine (red) and medieval/post-medieval (blue).

To corroborate the patterns of gene flow suggested by the f_4 -statistics, we used Treemix⁸⁴ to generate an admixture graph of all ancient rat populations, using the Asian house rat as an outgroup. The maximum-likelihood population tree without any admixture produced a similar topology to the neighbour-joining autosomal phylogeny (Supplementary Fig. 10). The rats from the northern group and a medieval Tunisian rat formed a clade, to which all the other Mediterranean rats were an outgroup, without any significant clustering pattern among the lineages. When admixture events were allowed, the first two suggested gene flow edges were from the medieval central European population into the post-medieval Buda Castle population, estimated to $18.2 \pm 3.0\%$, and from the Roman western European population into the ancestral lineage of the medieval European populations in the northern group, estimated to be $8.1 \pm 0.8\%$ (Fig. 4B).

The results from both the f_4 -statistics and Treemix analyses revealed a degree of Roman rat ancestry in the medieval populations. More specifically, medieval rats were more closely related to the Roman rat populations from the Netherlands and Britain (Fig. 4, Supplementary Data 4). This signal suggests a reservoir of black rat population in western Europe that admixed with the re-introduced medieval population. The stronger affinity of medieval western European populations to Roman populations (Supplementary Data 4) also suggested that this relict population was more likely distributed in western and not central Europe. This result could indicate that rats from the northernmost Roman provinces were not extirpated, despite their absence in early medieval zooarchaeological assemblages. Alternatively, and in our view more likely, the inferred relict population may have been located in an unsampled region of France or the Iberian Peninsula. The observation that medieval rats from temperate Europe fall into the same cluster as Roman rats also suggests that the second (medieval) wave of introduction to temperate Europe probably originated from the same source population as the first (Roman) dispersal. Considering the zooarchaeological evidence that rat populations in southern Europe persisted after the collapse of the Western Roman Empire, notably in Italy⁴⁰, it is likely that southern Europe was the source of reintroduced rats in temperate Europe.

Given the presence of rats in 9th century northern *emporium* (proto-urban trading sites) around the North and Baltic

Seas^{46,49,50}, a southern European origin would emphasise the importance of the Carolingian Empire (the Frankish polity which controlled much of western and central Europe as well as northern Italy in the 9th century CE) and routes such as the Rhône and Rhine corridors in reestablishing large-scale trade links between the Mediterranean and northern Europe⁸⁵. This connection remains tentative until samples from the early emporia themselves, mainland Italy, and the Iberian Peninsula can be investigated. Samples from the early Islamic world derived from the Iberian Peninsula and North Africa would also help to clarify the population history of black rats.

Discussion

This study explores the historic dispersal of commensal black rats using a de novo genome assembly for the black rat, ancient and modern mtDNA from across Europe, Africa, and the Indian Ocean, and ancient nuclear genomes from the Mediterranean and Europe. Our results confirm that the black rat was most likely introduced to the eastern Mediterranean by an overland route through Southwest Asia, though a maritime route via the Indian Ocean and Red Sea cannot be excluded. We identify two waves of rat introduction into temperate Europe. The first likely accompanied the Roman northward expansion during the first centuries BCE/CE and the second took place during the medieval period (starting in the 8th–10th centuries CE). The rats in this second wave were probably derived from the same ancestral population as the first, and subsequently admixed with a western or southern European relict population from the first wave.

Considered alongside the paucity of archaeological rat remains from the 6th to 8th centuries CE (particularly in northern and western Europe), this population turnover suggests that the black rat population and range declined during the early medieval period. This may have been associated with the breakdown of the Roman Empire—from the 5th century CE in western Europe and the early 7th century CE in the Balkans—and with it the network of well-connected settlements that had previously supported black rat populations. Grain shipments may have played a key role in the dispersal and maintenance of rat populations during the Roman period, and it is notable that weevils (*Sitophilus granarius*) and other grain pests show a similar pattern of Roman introduction, apparent

post-Roman extirpation, and a medieval reintroduction in the former northern provinces⁸⁶. Alternatively, or additionally, European rat populations may have been negatively impacted by the First Plague Pandemic and/or the climatic cooling of the Late Antique Little Ice Age, both of which began in the mid-6th century CE. To disentangle these scenarios, further zooarchaeological and genomic studies of ancient rats are required that span these centuries across a wider geographic range.

The medieval introduction of rats into Northern Europe is attested by their presence in Germany in the early 10th century (at the latest), coincident with an increase in the appearance of rat bones in archaeological contexts across the continent. Our results suggest a repopulation of temperate Europe from the south, perhaps linked with the development of trade routes in Carolingian western Europe, and probably not via early Russian riverine trade as has been previously hypothesised³². Black rats appear to have been a continuous presence in Europe from this point until the post-medieval period, spanning the 14th century Black Death and extending into the 17th century. This population may also have been supplemented by localised introductions, including one potentially associated with the Ottoman occupation of Buda from 1541 CE.

The recent dramatic decline in black rat populations across modern Europe, with local extirpation in much of the north of the continent, is likely linked to competition with the brown rat which arrived from Asia in the early 18th century^{52,53}. The genetic and demographic impact of this dispersal on black rats is an important area for future investigations since by the late 18th century, naturalists in many European countries had already attributed a marked decline in the black rat to competition from the brown rat^{87–90}. The black rat's significantly reduced, but persistent presence, particularly in towns, suggests a degree of niche partitioning between the two species⁹¹.

Our results reveal the degree to which human-commensal species can undergo population dispersal and demographic fluctuations. In fact, because these dynamic evolutionary processes are tightly correlated with the characteristics of the human niche, commensal species can act as ideal proxies to interpret the history of human movement and cultural change.

Methods

Ethics statement. Ethics board approval was not required for analysis of the black rat specimens since these were non-human and in most cases deceased upon collection. The exception, a modern black rat from California, was sourced from municipal pest control and humanely euthanized using a standard American Veterinary Medicine Association-approved method. In most cases, permits were not required for analysis of the ancient specimens, which were provided by co-authors on the paper who either excavated or already had access to the material. Specimens from Assos (Ass_1, Ass_2) were exported with the permission of the Çanakkale Museum, Turkey (77366169-152/766). Specimens from Rirha (AJ410-AJ414) were exported under a permit from the Ministry of Culture of Morocco. Rat bones from Panga Ya Saidi (AJ37-AJ38) and Chombo (AJ40-AJ41) were obtained and exported with permission from the National Council for Science and Technology, Kenya (Research Clearance Permit NCST/RRI/12/1/SS/541; Exploration/Excavation Licence NMK/GVT/2) and National Museums Kenya (export permit dated 12/09/2011). The sample from Songo Mnara (AJ40) was exported under permit EA.402/605/01/9 issued by the Antiquities Division, Ministry of Natural Resources and Tourism, Tanzania. Formal loan/sampling agreements were signed with: University of Tartu Archaeological Collection (samples AJ363, AJ366; Sampling Protocol #89), South Holland Provincial Archaeological Depot (samples AJ469-AJ472; loan number 2018-27), Åland Museum (samples AJ404-AJ409, ÅLR 2018/3788). Recent, non-archaeological specimens were sampled from existing museum collections.

Radiocarbon dating and calibration. Fourteen ancient rat bones were directly radiocarbon dated via accelerator mass spectrometry (AMS) on bone collagen at Mannheim (MAMS), University of Waikato (Wk), and Oxford University (OxA). These were analysed alongside two previously published dates from Gatehampton⁹² (Supplementary Data 3). One additional sample (SNE002/Wk-51521) failed due to insufficient collagen. All radiocarbon dates were calibrated in OxCal 4.4⁹³, using the IntCal20 calibration curve⁹⁴.

Given the omnivorous diet of black rats, stable isotope values were monitored for evidence of marine dietary contributions that might result in significant reservoir effects. Where possible, $\delta^{13}\text{C}$ (‰, VPDB) and $\delta^{15}\text{N}$ values (‰, AIR) were obtained by the respective dating laboratories using Isotope Ratio Mass Spectrometry (IRMS) and their standard protocols; otherwise $\delta^{13}\text{C}$ values were used as reported from the AMS. Nitrogen isotope values were available for 10 specimens and fell between 6.9‰ – 11.9‰, consistent with published data for commensal brown rats⁹⁵ and with an omnivorous diet. Carbon isotope values ranged from –21.9‰ to –17.4‰. In the absence of detailed local comparative isotope data from terrestrial and marine species, it was not possible confidently to estimate marine dietary contribution and hence the magnitude of any required correction. Nonetheless, we performed indicative corrections for specimens whose $\delta^{13}\text{C}$ values suggested a possible non-negligible marine component in order to test for any possible impact on our interpretations. The cut-off for this was set as –18.5‰, based on published values for European terrestrial herbivores and the enrichment expected due to trophic level in an omnivore.

For six specimens with $\delta^{13}\text{C} > -18.5\text{‰}$, percentage marine contribution was estimated using “formula 1” from⁹⁶, with terrestrial and marine endpoints of –21‰ and –12‰, respectively, and a trophic enrichment factor of 1‰. These values were used to recalibrate the dates using mixed IntCal20 and Marine20⁹⁷ curves, and the magnitude of potential offset was assessed. In no case did the median calibrated date change by more than 140 years, and in no case would it have moved a specimen into a different chronological category or altered our interpretations. Given the uncertainty inherent in this process, the uncorrected ranges are used in Fig. 3, and details of the indicative corrections are given in Supplementary Data 3. In the majority of cases, the uncorrected date range coincided more closely with the stratigraphic dating.

De novo genome assembly. The black rat genome was sequenced and assembled using DNA extracted from the liver of a male wild-caught individual from California, USA. Shotgun, Chicago and Dovetail Hi-C libraries were prepared and sequenced on Illumina HiSeq 4000 platform and the genome was assembled using Meraculous 2.2.5.1⁹⁸ and HiRise scaffolding pipeline⁶⁴. The detailed information of genome assembly is provided in the Supplementary Note 1.

The repetitive regions were identified using RepeatMasker 4.0.7⁹⁹ with Repbase 20170127 and the query species set as *rattus*, and TRF 4.09 (Tandem repeats finder)¹⁰⁰, with parameters set as “2 7 7 80 10 50 12”. The completeness of genome assembly was assessed by BUSCO 3.0.2⁶⁵, using the 303 orthologs in the Eukaryota odb9 dataset. The new genome assembly was aligned to the brown rat reference genome *Rnor_6.0* using nucmer 4.0.0 in MUMmer tool package¹⁰¹, to investigate the synteny between black rat and brown rat genomes, using both masked assemblies and anchor matches that are unique in both reference and query (Supplementary Note 1).

Mitochondrial Cytochrome B fragment sequencing. Overall, 292 tissue samples identified as the black rat were included for analysis, including 263 museum specimens (sampled from the collections at: American Museum of Natural History, Natural History Museum London, Field Museum Chicago) and 29 modern specimens collected in the field representing a wide geographic area at the periphery and on islands within the Indian Ocean.

DNA extraction and sequencing of these modern and museum samples were conducted in the modern laboratory at the Archaeology Department of Durham University, following standard protocols (Supplementary Note 4). The cytb region was amplified in 10 overlapping fragments and a variety of primer combinations was used depending on the nature of the sample (Supplementary Table 6). The sequencing reaction was carried out by the DNA Sequencing Service at the School of Biological and Biomedical Sciences at Durham University. The sequencing chromatograms were edited manually, subsequently assembled, and a consensus sequence per individual exported using Geneious R6 version 6.0.6 (<https://www.geneious.com>). Standard anti-contamination guidelines were followed. We successfully amplified cytb sequences from 202 of 292 samples. Only those that possessed >90% gene coverage were included in the analysis, which left 132 sequences.

Ancient DNA extraction and processing. We sampled 191 ancient black rats and eight modern black rat individuals from 33 archaeological sites across Europe and three sites in North Africa (Supplementary Note 3, Supplementary Data 2). Where multiple samples were taken from the same or related archaeological contexts, care was taken to ensure that these represented discrete individuals—either by sampling the same skeletal element and side, or on the basis of differing size and/or age.

Ancient DNA extraction was performed in dedicated ancient DNA facilities at the University of Oxford, the Max Planck Institute for the Science of Human History in Jena, and the University of York. All of the ancient lab facilities followed standard ancient DNA laboratory practices to minimise contamination, including the use of blanks at each stage from extraction to amplification. All material analysed at Oxford underwent the following treatment. Due to the small size of black rat bones, the outer surface of the bones was not removed prior to extraction. Bones that weighed <50 mg were completely consumed during the extraction process. The bone or tooth was cut using a Dremel drill with a clean cutting wheel

per sample (Dremel no. 409) and pulverised in a Micro-dismembrator (Sartorius-Stedim Biotech). Material analysed at York was subjected to bleach treatment (6% sodium hypochlorite for 5 min, and then rinsed with ultrapure water three times) prior to powdering following the same procedure as Oxford.

Extractions performed in Jena followed a silica-based protocol¹⁰² using 50 mg of bone powder. Extractions performed at the University of Oxford were conducted using the Dabney protocol with a modification of the addition of a 30 min pre-digestion stage¹⁰³. Extractions performed at the University of York were conducted using a silica-based protocol¹⁰⁴ modified to include a DNA concentration step using a centrifugal filter¹⁰⁵.

For each sample processed in Jena, a double-stranded DNA sequencing library was prepared from 20 µL of extract, with partial uracil-DNA-glycosylase (UDG) treatment (hereafter denoted as ds_halfUDG) or without UDG treatment (ds_nonUDG), following a published protocol¹⁰⁶. Sample-specific index combinations were added to the sequencing libraries^{107,108}. The indexed libraries were shotgun sequenced on an Illumina HiSeq 4000 instrument for screening, with 75 single-end-run cycles for ds_halfUDG libraries and 75 double-end-run cycles for ds_nonUDG libraries. After screening, one ds_nonUDG library and seven ds_halfUDG libraries were deep sequenced in the University of Kiel, on an Illumina HiSeq 4000 platform with 75 double-end-run cycles using the manufacturer's protocol.

All extracts generated at the University of Oxford and the University of York were built into Illumina libraries using double stranded methods using the Blunt-End Single-Tube Illumina library building (BEST) protocol as described previously¹⁰⁹ at the University of Oxford (ds_nonUDG). To amplify each library, 15 µL of library was added along with the following reagents: 25 µL of Accuprime Supermix I, 4 µL of BSA (10 mg/ml) and 3 µL of indexing primers 2 µM for a total volume of 50 µL. An additional barcode was added to the IS1_adapter.P5 adapter resulting in a double external indexed library. The libraries were then amplified on an Applied Biosystems StepOnePlus Real-Time PCR system, to determine both the success of the library build and the number of optimum cycles to use for the indexing PCR reactions. These 164 libraries were pooled at equimolar concentrations ready for sequencing. The pool of libraries was sequenced on an Illumina HiSeq 4000 (paired-end 75 bp) at the Danish National High-Throughput Sequencing Centre.

Ten extracts from Oxford were built into single-stranded libraries at the Max Planck Institute for Evolutionary Anthropology in Leipzig, Germany. The libraries were built from 30 µL of DNA extract in the absence of uracil DNA glycosylase (ss_nonUDG) followed by double indexing, using an automated version of the protocols described in^{107,108} on a liquid handling system (Agilent Technologies Bravo NGS Workstation). From the initial screening run results 31 ds_nonUDG libraries from Oxford were included for deeper sequencing in Jena, together with the ten ss_nonUDG libraries, on an Illumina HiSeq 4000 platform at the Max Planck Institute for the Science of Human History, Jena with 75 single-end-run cycles (Supplementary Data 2).

Genotyping and dataset preparation. After shotgun screening, we selected the samples for deeper sequencing based on their endogenous DNA content, selecting those with the highest percent endogenous DNA and the location and period of the sampling sites to ensure an even spread. These shotgun sequencing reads from 39 ancient and modern black rats were cleaned and mapped to the de novo black rat genome assembly using the EAGER pipeline 1.92.55¹¹⁰. Within the pipeline, the adapters were removed by AdapterRemoval 2.2.0¹¹¹, reads were mapped with BWA 0.7.12 aln/samse algorithm¹¹², duplications were removed by DeDup 0.12.1 (<https://github.com/apeltzer/DeDup>) and damage patterns of each library were checked with mapDamage 2.0.6¹¹³. For the seven ds_halfUDG libraries, we masked 2 bp from both ends of the reads using trimBam in bamUtil 1.0.13¹¹⁴ to remove the damaged sites.

The shotgun sequencing reads from four modern individuals, including the Californian black rat for de novo genome assembly, two published brown rat individuals (Accession: ERS215789, ERS215791)⁶⁷ and one published Asian house rat individual (Accession: SRS1581480, HXM4)¹¹⁵ were mapped to the genome assembly using the BWA 0.7.12 mem algorithm. After using a mapping quality filtering of 30 and removing reads with multiple hits, duplications were removed using DeDup. We then performed indel realignment for cleaned bam files of both ancient and modern individuals using RealignerTargetCreator and IndelRealigner in The Genome Analysis Toolkit (GATK) v3.5.0¹¹⁶.

For the demographic history analysis, we called diploid genotypes from three modern genomes using the highest coverage genome of each of the species: black rat (CP-5999), brown rat (ERS215791) and Asian house rat (HXM4). Each of the bam files was piled up using samtools mpileup, using reads with mapping quality and base quality over 30, and BAQ disabled. Bi-allelic SNPs were then individually called using bcftools call -m mode and filtered for SNPs with phred-scaled quality score (QUAL) over 30, sequence depth between 0.5–2X mean coverage, and not within 5 bp of an indel. After masking for repetitive regions, the consensus sequences of 18 largest autosomal scaffolds were generated, with heterozygous sites represented by IUPAC nucleotide code.

We called the pseudo-haploid genotypes in autosomal regions, from all modern and ancient individuals using ANGSD 0.931¹¹⁷, with parameter “-doHaploCall 1” to randomly sample one base. As the 18 longest autosomal scaffolds covered >99%

of the autosomal assembly, we only called genotypes on the non-repetitive regions of these 18 scaffolds. We applied “-remove_bads 1 -uniqueOnly 1 -minMapQ 30 -minQ 30 -C 50 -baq 1” parameters to filter out reads that had multiple hits, with mapping quality or base quality less than 30, perform base alignment quality (BAQ) computation and adjust mapping quality based for excessive mismatches¹¹⁸. To remove the deamination-induced damages in ancient DNA molecules, we only kept the transversion variants for downstream analysis. The genotypes on single-copied male-specific Y-chromosome regions (scpMSY) were called from all male individuals using ANGSD 0.931, with the same filters as autosomal genotyping, and -doHaploCall 2 to get the major call. The detailed information of scpMSY regions identification was provided in Supplementary Note 1.

To estimate the heterozygosity rates of ancient rat samples, the cleaned reads with base quality and mapping quality over 30 were piled up with mpileup in SAMtools 1.3¹¹⁹. We then called pseudo-diploid genotypes with pileupCaller 1.2.2 (<https://github.com/stschiff/sequenceTools>) under random diploid calling mode, which randomly sampled two reads at each site, on the transversion variants identified in ANGSD. The heterozygosity rates calculated from pseudo-diploid genotypes were half of the real heterozygosity rates of the samples on these variants.

The sequencing reads of all the screened black rats after AdapterRemoval were also mapped to black rat reference mitochondrial sequence NC_012374.1 with BWA 0.7.12 aln/samse algorithm and realigned with CircularMapper 1.0¹¹⁰. The reads of brown rat and Asian house rat individuals were mapped to mitochondrial references of the brown rat (NC_001665.2) and the Asian house rat (NC_011638.1), respectively. After removing duplication using DeDup, the consensus sequences were generated by Schmutzi with a quality threshold of 30¹²⁰. All the samples with <6000 missing sites in the consensus sequences were included in the downstream mitogenome analysis.

Demographic history analysis. The population size dynamics was estimated using PSMC 0.6.566, with parameter “-N25 -t20 -r5 -p “4 + 25*2 + 4 + 6”” and 100 bootstrap replicates. The PSMC output was visualised with generation time of 0.5 years and mutation rate $\mu = 2.96 \times 10^{-9}$ site/generation, based on an estimate calculated in a previous study of the brown rat⁶⁷.

G-PhoCS 1.2.3⁶⁸ was applied to estimate the population sizes, population divergence times and migration rates among three rat species, using the three high-coverage diploid genomes. The analysis was performed on 38,078 loci of 1 kb length, identified in non-repetitive, autosomal regions. A preliminary analysis with all possible migration events was first run for 250,000 generations, then two parallel runs for 500,000 generations with one migration event were carried out for parameter estimation. Finally, the estimated parameters were converted to effective population sizes (N_e), divergence times (T) and total migration rates (m_{total}) as described in⁶⁸: $\theta = 4 * N_e * \mu$, $\tau = T * \mu / g$ and $m_{total} = m * \tau$, with mutation rate $\mu = 2.96 \times 10^{-9}$ site/generation and generation time (g) of 0.5 years. The detailed information for loci selection and analysis was provided in Supplementary Note 2.

Phylogenetic analysis. The 67 ancient and 3 modern newly assembled mitochondrial genomes were analysed alongside seven modern reference genomes, including the modern Californian black rat from the reference genome assembly, two published brown rat individuals⁶⁷, one published Asian house rat individual¹¹⁵ and the published mitochondrial genome references of the three species (black rat NC_012374.1, Asian house rat NC_011638.1, brown rat NC_001665.2). The haplotypes were aligned using MUSCLE v3.8.1551¹²¹ with default parameters. Overall, 47 mitochondrial sequences from 77 individuals were involved in the analysis. The best-fit model was selected based on Akaike Information Criterion (AIC) calculated by jmodeltest v2.1.10¹²². The Maximum Likelihood (ML) tree was built using RAxML v8.2.12¹²³, with GTR + I + G model and 100 bootstrap replicates.

The cytb region of the mitochondrial genome haplotypes were extracted using MEGA7, and combined with modern cytb haplotypes from previous publications^{10,24,69,70} and this study. We aligned the data using MAFFT v7.123b¹²⁴, then built a ML tree using RAxML v8.2.9¹²³, with GTR + I + G model and 1000 bootstrap replicates.

The autosomal phylogeny was reconstructed using the neighbour-joining (NJ) method implemented in package Ape 5.3 in R 3.5.1, for 43 individuals, including 36 ancient black rats, 4 modern black rats, two brown rats, and one Asian house rat. The distance matrix was calculated based on 3,393,710 autosomal transversion variants, after removing singletons, using the genetic distance described in Gronau et al.⁶⁸. Bootstrapping was performed by resampling the variants from 100 kb non-overlapping windows, and the support on each node was calculated based on 100 bootstrap replicates. The phylogenetic tree based on Y-chromosome scpMSY regions was built with RAxML 8.2.12¹²³, using GTR substitution model, ML estimation of base frequencies and 100 rapid bootstrapping replicates.

Population genetics analysis. The IBS distance matrix among individuals was calculated using PLINK v1.90b¹²⁵ with parameter “-distance 1-ibs”. MDS analysis was performed using PLINK and ten dimensions were calculated on both datasets including all studied individuals and black rat individuals only. The f_4 -statistics

were calculated by *qpDstat* 755 in ADMIXTOOLS 5.1 package¹²⁶, with parameter “f4 mode: YES”, and the two brown rat individuals were used as the outgroup in all the analyses. The standard errors (SE) of f_4 -statistics were estimated using jackknife among autosomal scaffolds.

We also applied Treemix 1.13⁸⁴ to simultaneously infer the population structure and admixture events among black rat populations. The black rat samples were grouped based on the geographic location, time period and phylogenetic pattern identified in previous analysis (Supplementary Data 2). The allele frequency was calculated by PLINK and 1,145,713 sites covered in at least one sample from each group were included in the analysis. We built the admixture graph assuming 0–10 migration events, with parameters “-k 500 -global -se -noss -root tanezumi” to group 500 SNPs per block for covariance matrix estimation. We then performed a global rearrangement after adding all the populations, calculated standard errors of migration weights, disabled sample size correction and assigned the Asian house rat as the root of the topology.

Reporting summary. Further information on research design is available in the Nature Research Reporting Summary linked to this article.

Data availability

The black rat genome assembly is available in the NCBI under the accession number [GCA_011800105.1](https://www.ncbi.nlm.nih.gov/assembly/GCA_011800105.1). Aligned reads from the 39 newly reported ancient and modern black rats are available at the ENA archive under the accession number [PRJEB47337](https://www.ebi.ac.uk/ena/record/PRJEB47337). The mitochondrial haplotypes are available at NCBI GenBank under the accession number [OK210796-OK210933](https://www.ncbi.nlm.nih.gov/nuccore/OK210796-OK210933) for CYTB regions and [OM574930-OM574970](https://www.ncbi.nlm.nih.gov/nuccore/OM574930-OM574970) for mitochondrial genomes. Source data are provided as a Source Data file, with Supplementary Data 1 and 4.

Received: 27 April 2021; Accepted: 18 March 2022;

Published online: 03 May 2022

References

- Boivin, N. L. et al. Ecological consequences of human niche construction: Examining long-term anthropogenic shaping of global species distributions. *Proc. Natl Acad. Sci. USA* **113**, 6388–6396 (2016).
- Capizzi, D., Bertolino, S. & Mortelliti, A. Rating the rat: global patterns and research priorities in impacts and management of rodent pests. *Mamm. Rev.* **44**, 148–162 (2014).
- Meerburg, B. G., Singleton, G. R. & Kijlstra, A. Rodent-borne diseases and their risks for public health. *Crit. Rev. Microbiol.* **35**, 221–270 (2009).
- McCormick, M. Rats, communications, and plague: toward an ecological history. *J. Interdiscip. Hist.* **34**, 1–25 (2003).
- Aplin, K. P., Brown, P., Jacob, J., Krebs, C. J. & Singleton, G. R. *Field Methods for Rodent Studies in Asia and the Indo-Pacific* (Australian Centre for International Agricultural Research, 2003).
- Lack, J. B. et al. Invasion facilitates hybridization with introgression in the *Rattus rattus* species complex. *Mol. Ecol.* **21**, 3545–3561 (2012).
- Conroy, C. J. et al. Cryptic genetic diversity in *Rattus* of the San Francisco Bay region, California. *Biol. Invasions* **15**, 741–758 (2013).
- Robins, J. H., Hingston, M., Matisoo-Smith, E. & Ross, H. A. Identifying *Rattus* species using mitochondrial DNA. *Mol. Ecol. Notes* **7**, 717–729 (2007).
- Pagès, M. et al. Revisiting the taxonomy of the Rattini tribe: a phylogeny-based delimitation of species boundaries. *BMC Evol. Biol.* **10**, 184 (2010).
- Aplin, K. P. et al. Multiple geographic origins of commensalism and complex dispersal history of Black Rats. *PLoS ONE* **6**, e26357 (2011).
- Robins, J. H. et al. Dating of divergences within the *Rattus* genus phylogeny using whole mitochondrial genomes. *Mol. Phylogenet. Evol.* **49**, 460–466 (2008).
- Yosida, T. H., Kato, H., Tsuchiya, K. & Moriwaki, K. Karyotypes and serum transferrin patterns of hybrids between Asian and Oceanian black rats, *Rattus rattus*. *Chromosoma* **34**, 40–50 (1971).
- Hulme-Beaman, A., Dobney, K., Cucchi, T. & Searle, J. B. An ecological and evolutionary framework for commensalism in anthropogenic environments. *Trends Ecol. Evol.* **31**, 633–645 (2016).
- Jones, E. P., Eager, H. M., Gabriel, S. I., Jóhannesdóttir, F. & Searle, J. B. Genetic tracking of mice and other bioproxies to infer human history. *Trends Genet.* **29**, 298–308 (2013).
- Puckett, E. E., Orton, D. & Munshi-South, J. Commensal rats and humans: integrating rodent phylogeography and zooarchaeology to highlight connections between human societies. *Bioessays* **42**, e1900160 (2020).
- Jones, E. P. et al. Fellow travellers: a concordance of colonization patterns between mice and men in the North Atlantic region. *BMC Evol. Biol.* **12**, 35 (2012).
- Cucchi, T. Uluburun shipwreck stowaway house mouse: molar shape analysis and indirect clues about the vessel’s last journey. *J. Archaeol. Sci.* **35**, 2953–2959 (2008).
- Cucchi, T. et al. On the trail of Neolithic mice and men towards Transcaucasia: zooarchaeological clues from Nakhchivan (Azerbaijan). *Biol. J. Linn. Soc. Lond.* **108**, 917–928 (2013).
- Cucchi, T. et al. Tracking the Near Eastern origins and European dispersal of the western house mouse. *Sci. Rep.* **10**, 8276 (2020).
- Matisoo-Smith, E. & Robins, J. H. Origins and dispersals of Pacific peoples: evidence from mtDNA phylogenies of the Pacific rat. *Proc. Natl Acad. Sci. USA* **101**, 9167–9172 (2004).
- Matisoo-Smith, E. & Robins, J. Mitochondrial DNA evidence for the spread of Pacific rats through Oceania. *Biol. Invasions* **11**, 1521–1527 (2009).
- West, K. et al. The Pacific Rat Race to Easter Island: tracking the prehistoric dispersal of *Rattus exulans* using ancient mitochondrial genomes. *Front. Ecol. Evol.* **5**, 52 (2017).
- Niethammer, V. J. Zur Taxonomie und Ausbreitungsgeschichte der Hausratte (*Rattus rattus*). *Zool. Anz. Jena* **194**, 405–415 (1975).
- Baig, M., Khan, S., Eager, H., Atkulwar, A. & Searle, J. B. Phylogeography of the black rat *Rattus rattus* in India and the implications for its dispersal history in Eurasia. *Biol. Invasions* **21**, 417–433 (2019).
- Tchernov, E. Commensal animals and human sedentism in the Middle East. *Anim. Archaeol.* **3**, 91–115 (1984).
- Ervynck, A. Sedentism or urbanism? On the origin of the commensal black rat (*Rattus rattus*). In *Bones and the Man: Studies in Honour of Don Brothwell* (eds Dobney, K. & O’Connor, T. P.) 95–109 (Oxbow, 2002).
- Ruffino, L. & Vidal, E. Early colonization of Mediterranean islands by *Rattus rattus*: a review of zooarchaeological data. *Biol. Invasions* **12**, 2389–2394 (2010).
- Vigne, J.-D. & Valladas, H. E. Small mammal fossil assemblages as indicators of environmental change in Northern Corsica during the last 2500 years. *J. Archaeol. Sci.* **23**, 199–215 (1996).
- Oueslati, T. et al. 1st century BCE occurrence of chicken, house mouse and black rat in Morocco: socio-economic changes around the reign of Juba II on the site of Rirha. *J. Archaeol. Sci.: Rep.* **29**, 102162 (2020).
- Audoin-Rouzeau, F. & Vigne, J.-D. La colonisation de l’Europe par le rat noir (*Rattus rattus*). *Rev. Paléobiol.* **13**, 125–145 (1994).
- Audoin-Rouzeau, F. & Vigne, E. T. J.-D. Le rat noir (*Rattus rattus*) en Europe Antique et médiévale: les voies du commerce et l’expansion de la peste. *Anthropozoologica* **25/26**, 399–404 (1997).
- Armitage, P. L. Unwelcome companions: ancient rats reviewed. *Antiquity* **68**, 231–240 (1994).
- Hufthammer, A. K. & Walløe, L. Rats cannot have been intermediate hosts for *Yersinia pestis* during medieval plague epidemics in Northern Europe. *J. Archaeol. Sci.* **40**, 1752–1759 (2013).
- Dean, K. R. et al. Human ectoparasites and the spread of plague in Europe during the Second Pandemic. *Proc. Natl Acad. Sci. USA* **115**, 1304–1309 (2018).
- Sloane, B. *The Black Death in London* (The History Press, 2011).
- Hardy, A. The under-appreciated rodent: harbingers of plague from the middle ages to the twenty-first century. *J. Interdiscip. Hist.* **50**, 171–185 (2019).
- White, L. A. & Mordechai, L. Modeling the Justinianic Plague: comparing hypothesized transmission routes. *PLoS One* **15**, e0231256 (2020).
- O’Connor, T. P. On the lack of bones of the ship rat *Rattus rattus* from Dark Age York. *J. Zool.* **224**, 318–320 (1991).
- Rielly, K. The black rat. In *Extinctions and Invasions: a Social History of British fauna* (eds O’Connor, T. & Sykes, N.) 134–145 (Oxbow, 2010).
- Salvadori, F. The transition from late antiquity to early Middle Ages in Italy. A zooarchaeological perspective. *Quat. Int.* <https://doi.org/10.1016/j.quaint.2018.06.040> (2018).
- De Cupere, B. et al. Eagle owl (*Bubo bubo*) pellets from Roman Sagalassos (SW Turkey): distinguishing the prey remains from nest and roost sites. *Int. J. Osteoarchaeol.* **19**, 1–22 (2009).
- Parfitt, S. A. The small mammals. In *The Transition To Late Antiquity on the Danube and Beyond* (ed. Poulter, A. G.) 198–318 (Oxford University Press, 2007).
- Davis, E. M. Paleocological studies at Stobi. In *Studies in the Antiquities of Stobi*, Vol. 3 (eds Aleksova, B., Wiseman, J. & Mano-Zisi, Đ.) (Princeton University Press, 1981).
- Baron, H., Reuter, A. E. & Marković, N. Rethinking ruralization in terms of resilience: subsistence strategies in sixth-century Caričin Grad in the light of plant and animal bone finds. *Quat. Int.* **499**, 112–128 (2019).
- Benedictow, O. J. *What Disease was Plague?: On the Controversy Over the Microbiological Identity of Plague Epidemics of the Past* (Brill, 2010).
- O’Connor, T. P. *Bones from Anglo-Scandinavian levels at 16–22 Coppergate*. (Council for British Archaeology, 1989).
- Pasda, K. *Tierknochen als Spiegel sozialer Verhältnisse im 8.-15. Jh. in Bayern* (Prähistorica Verlag, 2004).

48. Dobney, K., Jacques, D., Barrett, J. & Johnstone, C. *Farmers, Monks and Aristocrats: the Environmental Archaeology of Anglo-Saxon Flixborough* (Oxbow, 2007).
49. Reichstein, H. *Die wildlebenden Säugetiere von Haithabu: Ausgrabungen 1966–1969 und 1979–1980.* (Karl Wachholtz, 1991).
50. Wigh, B. *Animal husbandry in the Viking Age town of Birka and its hinterland: excavations in the black earth 1990–95* (Riksantikvarieämbetet, 2001).
51. Tourunen, A. *Animals in an Urban Context—A Zooarchaeological Study of the Medieval and Post-Medieval town of Turku* (University of Turku, 2008).
52. Eryvncq, A. *Archeozoologisch onderzoek van de zwarte rat (*Rattus rattus*) en de bruine rat (*Rattus norvegicus*)* (Doctoral thesis, Amsterdam, 1989).
53. Barrett-Hamilton, G. & Hinton, M. A *History of British Mammals* (Gurney and Jackson, 1910).
54. Mitchell-Jones, A. J. et al. *The Atlas of European Mammals* (Poyser, 1999).
55. Savinetsky, A. B. & Krylovich, O. A. On the history of the spread of the black rat (*Rattus rattus* L., 1758) in northwestern Russia. *Biol. Bull. Russ. Acad. Sci.* **38**, 203–207 (2011).
56. Ward-Perkins, B. *The Fall of Rome and the End of Civilization* (Oxford University Press, 2005).
57. Wickham, C. *Framing the Early Middle Ages: Europe and the Mediterranean 400–800* (Oxford University Press, 2005).
58. Horden, P. & Purcell, N. *The Corrupting Sea: A Study of Mediterranean History* (Wiley-Blackwell, 2000).
59. Ambrosiani, B. Osten und Westen im Ostseehandel zur Wikingerzeit. In *Haithabu und die frühe Stadtentwicklung im nördlichen Europa* (eds Brandt, K., Müller-Wille, M. & Radtke, C.) 339–348 (Wachholtz, 2002).
60. Hodges, R. *Dark Age Economics: A New Audit* (Bloomsbury, 2012).
61. Keller, M. et al. Ancient *Yersinia pestis* genomes from across Western Europe reveal early diversification during the First Pandemic (541–750). *Proc. Natl Acad. Sci. USA* **116**, 12363–12372 (2019).
62. Wagner, D. M. et al. *Yersinia pestis* and the Plague of Justinian 541–543 AD: a genomic analysis. *Lancet Infect. Dis.* **14**, 319–326 (2014).
63. Feldman, M. et al. A high-coverage *Yersinia pestis* genome from a sixth-century Justinianic Plague victim. *Mol. Biol. Evol.* **33**, 2911–2923 (2016).
64. Putnam, N. H. et al. Chromosome-scale shotgun assembly using an in vitro method for long-range linkage. *Genome Res.* **26**, 342–350 (2016).
65. Simão, F. A., Waterhouse, R. M., Ioannidis, P., Kriventseva, E. V. & Zdobnov, E. M. BUSCO: assessing genome assembly and annotation completeness with single-copy orthologs. *Bioinformatics* **31**, 3210–3212 (2015).
66. Li, H. & Durbin, R. Inference of human population history from individual whole-genome sequences. *Nature* **475**, 493–496 (2011).
67. Deinum, E. E. et al. Recent evolution in *Rattus norvegicus* is shaped by declining effective population size. *Mol. Biol. Evol.* **32**, 2547–2558 (2015).
68. Gronau, I., Hubisz, M. J., Gulko, B., Danko, C. G. & Siepel, A. Bayesian inference of ancient human demography from individual genome sequences. *Nat. Genet.* **43**, 1031–1034 (2011).
69. Colangelo, P. et al. Mitochondrial phylogeography of the black rat supports a single invasion of the western Mediterranean basin. *Biol. Invasions* **17**, 1859–1868 (2015).
70. Etougbéché, J. et al. Genetic diversity and origins of invasive black rats (*Rattus rattus*) in Benin, West Africa. *fozo* **1** 69, 20014.1 (2020).
71. Hemamali, P. P. C. & Boyagoda, S. H. Historic black rat invasions into Sri Lanka lead to hybridization forming two sub-lineages in the *Rattus rattus* species complex. *Ceylon J. Sci.* **49**, 433 (2020).
72. Carleton, G. G., Musserand, M. D. & Musser, G. G. Superfamily Muroidea. In *Mammal Species of the World: A Taxonomic and Geographic Reference* 3rd edn (eds Wilson, D. E. & Reeder, D. M.) 894–1531 (Johns Hopkins University Press, 2005).
73. Boivin, N. Proto-globalisation and biotic exchange in the old world. In *Human Dispersal and Species Movement from Prehistory to the Present* (eds Boivin, N., Crassard, R. & Petraglia, M.) 349–408 (Cambridge University Press, 2017).
74. Cooper, J. P. Egypt's Nile-Red Sea canals: chronology, location, seasonality and function. In *Red Sea IV: Connected Hinterlands* (eds Blue, L., Cooper, J., Thomas, R. & Whitewright, J.) 195–210 (Archaeopress, 2009).
75. Prendergast, M. E. et al. Reconstructing Asian faunal introductions to eastern Africa from multi-proxy biomolecular and archaeological datasets. *PLoS ONE* **12**, e0182565 (2017).
76. Tollenaere, C. et al. Phylogeography of the introduced species *Rattus rattus* in the western Indian Ocean, with special emphasis on the colonization history of Madagascar. *J. Biogeogr.* **37**, 398–410 (2010).
77. Cobb, M. The chronology of Roman Trade in the Indian Ocean from Augustus to early third century ce. *J. Econ. Soc. Hist. Orient* **58**, 362–418 (2015).
78. Ewer, R. F. The biology and behaviour of a free-living population of black rats (*Rattus rattus*). *Anim. Behav. Monogr.* **4**, 127–174 (1971).
79. Pocock, M. J. O., Hauffe, H. C. & Searle, J. B. Dispersal in house mice. *Biol. J. Linn. Soc. Lond.* **84**, 565–583 (2005).
80. Büntgen, U. et al. Cooling and societal change during the Late Antique Little Ice Age from 536 to around 660 AD. *Nat. Geosci.* **9**, 231–236 (2016).
81. Perry, R. D. & Fetherston, J. D. *Yersinia pestis*-etiologic agent of plague. *Clin. Microbiol. Rev.* **10**, 35–66 (1997).
82. Spyrou, M. A., Bos, K. I., Herbig, A. & Krause, J. Ancient pathogen genomics as an emerging tool for infectious disease research. *Nat. Rev. Genet.* **20**, 323–340 (2019).
83. Fenwick, C. From Africa to Ifriqiya: settlement and society in early Medieval North Africa (650–800). *Al-Masāq* **25**, 9–33 (2013).
84. Pickrell, J. K. & Pritchard, J. K. Inference of population splits and mixtures from genome-wide allele frequency data. *PLoS Genet.* **8**, e1002967 (2012).
85. McCormick, M. Where do trading towns come from? Early medieval Venice and the northern emporia. *Post-Rom. towns, trade Settl. Eur. Byzantium* **1**, 41–68 (2007).
86. Smith, D. & Kenward, H. Roman grain pests in Britain: implications for grain supply and agricultural production. *Britannia* **42**, 243–262 (2011).
87. Buffon, G.-L. L. C. de. *Histoire Naturelle, Générale et Particulière, avec la Description du Cabinet du Roi*, Vol. 8 (L'Imprimerie Royale, 1760).
88. Smith, R. *The Universal Directory for Taking Alive and Destroying Rats, and All Other Kinds of Four-footed and Winged Vermin, In a Method Hitherto Unattempted: Calculated for the Use of the Gentleman, the Farmer, and the Warrener* (J. Walker, 1768).
89. Pennant, T. *British Zoology* (William Eyres, 1776).
90. Ruttly, J. *An Essay Towards a Natural History of the County of Dublin*, Vol. 1 (W. Sleater, 1772).
91. O'Connor, T. Commensal species. In *The Oxford Handbook of Animal Studies* (ed. Kalof, L.) (Oxford University Press, 2017).
92. Walker, T., Sharpe, J. R. & Williams, H. Barn owls and black rats from a rural Roman Villa at Gatehampton, South Oxfordshire. *Environ. Archaeol.* **26**, 487–496 (2021).
93. Ramsey, C. B. Bayesian analysis of radiocarbon dates. *Radiocarbon* **51**, 337–360 (2009).
94. Reimer, P. J., Austin, W. E. N., Bard, E. & Bayliss, A. The IntCal20 northern hemisphere radiocarbon age calibration curve (0–55 cal BP). *Radiocarbon* **62**, 725–757 (2020).
95. Guiry, E. & Buckley, M. Urban rats have less variable, higher protein diets. *Proc. R. Soc. B* **285**, 20181441 (2018).
96. Dewar, G. & Pfeiffer, S. Approaches to estimating marine protein in human collagen for radiocarbon date calibration. *Radiocarbon* **52**, 1611–1625 (2010).
97. Heaton, T. J. et al. Marine20—the marine Radiocarbon Age calibration curve (0–55,000 cal BP). *Radiocarbon* **62**, 779–820 (2020).
98. Chapman, J. A. et al. Meraculous: de novo genome assembly with short paired-end reads. *PLoS ONE* **6**, e23501 (2011).
99. Smit, AFA, Hubley, R & Green, P. RepeatMasker Open-4.0. <http://www.repeatmasker.org> (2013–2015).
100. Benson, G. Tandem repeats finder: a program to analyze DNA sequences. *Nucleic Acids Res.* **27**, 573–580 (1999).
101. Kurtz, S. et al. Versatile and open software for comparing large genomes. *Genome Biol.* **5**, R12 (2004).
102. Dabney, J. et al. Complete mitochondrial genome sequence of a Middle Pleistocene cave bear reconstructed from ultrashort DNA fragments. *Proc. Natl Acad. Sci. USA* **110**, 15758–15763 (2013).
103. Damgaard, P. B. et al. Improving access to endogenous DNA in ancient bones and teeth. *Sci. Rep.* **5**, 11184 (2015).
104. Yang, D. Y., Eng, B., Wayne, J. S., Dudar, J. C. & Saunders, S. R. Technical note: improved DNA extraction from ancient bones using silica-based spin columns. *Am. J. Phys. Anthropol.* **105**, 539–543 (1998).
105. Speller, C. F. et al. Ancient mitochondrial DNA analysis reveals complexity of indigenous North American Turkey domestication. *Proc. Natl Acad. Sci. USA* **107**, 2807–2812 (2010).
106. Rohland, N., Harney, E., Mallick, S., Nordenfelt, S. & Reich, D. Partial uracil-DNA-glycosylase treatment for screening of ancient DNA. *Philos. Trans. R. Soc. Lond. B Biol. Sci.* **370**, 20130624 (2015).
107. Gansauge, M.-T., Aximu-Petri, A., Nagel, S. & Meyer, M. Manual and automated preparation of single-stranded DNA libraries for the sequencing of DNA from ancient biological remains and other sources of highly degraded DNA. *Nat. Protoc.* <https://doi.org/10.1038/s41596-020-0338-0> (2020).
108. Kircher, M., Sawyer, S. & Meyer, M. Double indexing overcomes inaccuracies in multiplex sequencing on the Illumina platform. *Nucleic Acids Res.* **40**, e3 (2012).
109. Carøe, C. et al. Single-tube library preparation for degraded DNA. *Methods Ecol. Evol.* **9**, 410–419 (2018).
110. Peltzer, A. et al. EAGER: efficient ancient genome reconstruction. *Genome Biol.* **17**, 60 (2016).
111. Schubert, M., Lindgreen, S. & Orlando, L. AdapterRemoval v2: rapid adapter trimming, identification, and read merging. *BMC Res. Notes* **9**, 88 (2016).
112. Li, H. & Durbin, R. Fast and accurate short read alignment with Burrows–Wheeler transform. *Bioinformatics* **25**, 1754–1760 (2009).

113. Jónsson, H., Ginolhac, A., Schubert, M., Johnson, P. L. F. & Orlando, L. mapDamage2.0: fast approximate Bayesian estimates of ancient DNA damage parameters. *Bioinformatics* **29**, 1682–1684 (2013).
114. Jun, G., Wing, M. K., Abecasis, G. R. & Kang, H. M. An efficient and scalable analysis framework for variant extraction and refinement from population-scale DNA sequence data. *Genome Res.* **25**, 918–925 (2015).
115. Teng, H. et al. Population genomics reveals speciation and introgression between Brown Norway rats and their sibling species. *Mol. Biol. Evol.* **34**, 2214–2228 (2017).
116. McKenna, A. et al. The Genome Analysis Toolkit: a MapReduce framework for analyzing next-generation DNA sequencing data. *Genome Res.* **20**, 1297–1303 (2010).
117. Korneliussen, T. S., Albrechtsen, A. & Nielsen, R. ANGSD: analysis of next generation sequencing data. *BMC Bioinforma.* **15**, 356 (2014).
118. Li, H. Improving SNP discovery by base alignment quality. *Bioinformatics* **27**, 1157–1158 (2011).
119. Li, H. et al. The Sequence Alignment/Map format and SAMtools. *Bioinformatics* **25**, 2078–2079 (2009).
120. Renaud, G., Slon, V., Duggan, A. T. & Kelso, J. Schmutzi: estimation of contamination and endogenous mitochondrial consensus calling for ancient DNA. *Genome Biol.* **16**, 224 (2015).
121. Edgar, R. C. MUSCLE: multiple sequence alignment with high accuracy and high throughput. *Nucleic Acids Res.* **32**, 1792–1797 (2004).
122. Darriba, D., Taboada, G. L., Doallo, R. & Posada, D. jModelTest 2: more models, new heuristics and parallel computing. *Nat. Methods* **9**, 772 (2012).
123. Stamatakis, A. RAxML version 8: a tool for phylogenetic analysis and post-analysis of large phylogenies. *Bioinformatics* **30**, 1312–1313 (2014).
124. Katoh, K. & Standley, D. M. MAFFT multiple sequence alignment software version 7: improvements in performance and usability. *Mol. Biol. Evol.* **30**, 772–780 (2013).
125. Purcell, S. et al. PLINK: a tool set for whole-genome association and population-based linkage analyses. *Am. J. Hum. Genet.* **81**, 559–575 (2007).
126. Patterson, N. et al. Ancient admixture in human history. *Genetics* **192**, 1065–1093 (2012).

Acknowledgements

We thank the wet laboratory teams at MPI-SHH, the PalaeoBARN at the University of Oxford and BioArch at the University of York. We thank David K. James and Lucia Hui of the Alameda County Vector Control Services District for procuring the rat used for the de novo genome. We are grateful to Sarah Nagel at Max Planck Institute for Evolutionary Anthropology for the single-stranded library preparation, and Dovetail Genomics for the de novo genome assembly service. We thank Maria Spyrou for her suggestions and comments. We acknowledge Ewan Chipping and Helena England (University of York), Carl Phillips, Veronica Lindholm (Ålands Museum), Christine McDonnell and Nienke van Doorn (York Archaeological Trust), Emile Mittendorf (Gemeente Deventer), Inge Riemersma (Archaeological depot, Provincie Zuid-Holland), the Turkish Ministry of Culture & Tourism and the Çanakkale Museum, Jan Frolík and Iva Herichová (Institute of Archaeology of the Czech Academy of Sciences, Prague), Franz Humer and Eduard Pollhammer (Archaeological Park Carnuntum), Dorottya B. Nyékelyi and László Daróczy-Szabó (Budapest History Museum), Institut National du Patrimoine (Tunisia), University of Barcelona, Spanish Ministry of Science and Innovation (Project HUM2006-03432/HIST), Spanish Ministry of Culture (programme of archaeological excavations abroad 2009), Spanish Agency of International Cooperation for the Development (2009), Catalan Institute of Classical Archaeology (ICAC), Vila Franca Municipal Museum and N'Zinga Oliveira (University of the Azores), Vujadin Ivanisević and Ivan Bugarski (Institute of Archaeology, Belgrade), Martin Nadler, M.A. and Dr. Silvia Codreanu-Windauer (Nürnberg and Regensburg respectively, Bavarian State Office for the Preservation of Monuments), the Field Museum of Natural History Chicago, The Natural History Museum London, and the American Museum of Natural History for providing

materials and support. Funding was provided by the European Research Council (ERC-StG-337574-UNDEAD to G.L.; ERC-StG-206148 to N.B.; ERC-StG-716298 to S.V.-L.), the Natural Environment Research Council Doctoral Training Programme (A.J.), Wellcome (Small Grant in Humanities and Social Science 209817/Z to D.O.), the British Academy/Leverhulme Trust (SG170938 to D.O.), Estonian Research Council (PRG29 to E.R.), Czech Academy of Sciences (RVO:67985912 to R.K.) and Leverhulme Trust (ECF-2017-315 to A.H.B.), National Science Foundation (BCS 1123091 to J.F./S.W.-J.), Arts and Humanities Research Council (AH/J502716/1 to S.W.-J./J.F.). The de novo genome assembly, population genomics study, and radiocarbon dating were funded by the Max Planck Society.

Author contributions

J.K., G.L. and D.O. designed the project; A.J., B.K.-K., B.K., C.S., H.A.-J., H.E., A.T. generated data; H.Y., A.J. and D.O. analysed data; G.A., N.B., H.B., B.B.-A., W.B., A.C., C.J.C., T.C., K.D., K.E., J.F., L.G., E.G., P.G., S.G., S.H.-D., C.H., R.H., N.K., H.K., Z.K., K.K., R.K., A.L., B.M.-T., N.M., A.M.-M., M.N., T.O'C., T.Ou, E.Q.M., K.P., J.P., N.P., S.R., J.R., E.R., J.B.S., J.S.G., E.T., S.V.-L., Ivan der J., W.V.N., J.-D.V., T.W., S.W.-J. and J.Z. provided material and support; H.Y., D.O., A.J., A.H.-B., G.L. and J.K. wrote the paper with contributions from all other authors.

Funding

Open Access funding enabled and organized by Projekt DEAL.

Competing interests

The authors declare no competing interests.

Additional information

Supplementary information The online version contains supplementary material available at <https://doi.org/10.1038/s41467-022-30009-z>.

Correspondence and requests for materials should be addressed to Johannes Krause, Greger Larson or David Orton.

Peer review information *Nature Communications* thanks the anonymous reviewer(s) for their contribution to the peer review of this work. Peer reviewer reports are available.

Reprints and permission information is available at <http://www.nature.com/reprints>

Publisher's note Springer Nature remains neutral with regard to jurisdictional claims in published maps and institutional affiliations.



Open Access This article is licensed under a Creative Commons Attribution 4.0 International License, which permits use, sharing, adaptation, distribution and reproduction in any medium or format, as long as you give appropriate credit to the original author(s) and the source, provide a link to the Creative Commons license, and indicate if changes were made. The images or other third party material in this article are included in the article's Creative Commons license, unless indicated otherwise in a credit line to the material. If material is not included in the article's Creative Commons license and your intended use is not permitted by statutory regulation or exceeds the permitted use, you will need to obtain permission directly from the copyright holder. To view a copy of this license, visit <http://creativecommons.org/licenses/by/4.0/>.

© The Author(s) 2022

¹Department of Archaeogenetics, Max Planck Institute for Evolutionary Anthropology, 04103 Leipzig, Germany. ²School of Life Sciences, Peking University, 100871 Beijing, China. ³Department of Archaeogenetics, Max Planck Institute for the Science of Human History, 07745 Jena, Germany. ⁴Palaeogenomics & Bio-Archaeology Research Network, Research Laboratory for Archaeology and History of Art, University of Oxford, Oxford OX1 3QY, UK. ⁵Department of Archaeology, Classics and Egyptology, University of Liverpool, Liverpool L69 7WZ, UK. ⁶Research Centre in Evolutionary Anthropology and Palaeoecology, Liverpool John Moores University, Liverpool L3 3AF, UK. ⁷Museum of Vertebrate Zoology, University of California, Berkeley, Berkeley, CA 94720-3160, USA. ⁸Department of Archaeology, University of York, York YO1 7EP, UK. ⁹BioArCh, Department of Archaeology, University of York, York YO1 7EP, UK. ¹⁰Department of Anthropology, University of British Columbia, Vancouver, BC, Canada. ¹¹Department of Ecology and Evolutionary Biology, Cornell University, Ithaca, NY 14853, USA. ¹²Charité – Universitätsmedizin Berlin, Institut für Pathologie, Charitéplatz 1, 10117 Berlin, Germany. ¹³Postgraduate Institute of Archaeology, 407, Bauddhaloka Mawatha, Colombo 7, Sri Lanka. ¹⁴Römisch-Germanisches Zentralmuseum, Leibniz-Forschungsinstitut für Archäologie, Ernst-Ludwig-Platz 2, 55116 Mainz, Germany. ¹⁵Christian Archaeology and Byzantine Art History, Philipps University of Marburg, 35037 Marburg, Germany. ¹⁶Department of History and Archaeology, University of Ruhuna, Matara 81000, Sri Lanka. ¹⁷Department of Archaeology,

Max Planck Institute for the Science of Human History, 07745 Jena, Germany. ¹⁸School of Social Science, The University of Queensland, St Lucia, QLD, Australia. ¹⁹Archaeozoology, Archaeobotany, Societies, Practices, Environments (AASPE-UMR7209), CNRS, National Museum of Natural History (MNHN), Paris, France. ²⁰Archeoplan Eco, 2616 LZ Delft, Netherlands. ²¹Department of Anthropology, Rice University, 6100 Main St, Houston, TX 77005, USA. ²²Archaeological Services, University of Durham, Durham, UK. ²³Ukrainian Scientific Center of Ecology of the Sea, Odessa 65009, Ukraine. ²⁴Schmalhausen Institute of Zoology, National Academy of Sciences of Ukraine, Kyiv 01030, Ukraine. ²⁵Negaunee Integrative Research Center, Field Museum of Natural History, Chicago, IL 60605, USA. ²⁶Department of Archaeology & Anthropology, Bournemouth University (Visiting Fellow), Poole BH12 5BB, UK. ²⁷Canterbury Archaeological Trust, 92a Broad Street, Canterbury, Kent CT1 2LU, UK. ²⁸6 Fell View Park, Gosforth, Seascale, Cumbria CA20 1HY, UK. ²⁹L'Ecole Tunisienne de l'Histoire et l'Anthropologie, Tunis, Tunisia. ³⁰University of Tunis, Tunis, Tunisia. ³¹Department of Culture, University of Helsinki, P.O. Box 59, FI-00014 Helsinki, Finland. ³²Osteological Research Laboratory, University of Stockholm, 10691 Stockholm, Sweden. ³³Freelance archaeozoologist, Liliom u. 4. 1/1, Balatonfüred 8230, Hungary. ³⁴VIAS Vienna Institute for Archaeological Science, University of Vienna, Althanstraße 14, 1090 Vienna, Austria. ³⁵Department of Natural Sciences and Archaeometry, Institute of Archaeology of the Czech Academy of Sciences, Prague, Letenská 4, 118 01, Prague, Czech Republic. ³⁶Centre for Palaeogenetics & Department of Geological Sciences, Stockholm University, Stockholm 10691, Sweden. ³⁷Institut National de Patrimoine, Tunis 1008, Tunisia. ³⁸Institute of Archaeology, 11000 Belgrade, Serbia. ³⁹Departamento de Biología, Universidad Autónoma de Madrid, 28049 Madrid, Spain. ⁴⁰Institute of Archaeology, University College London, London WC1H 0PY, UK. ⁴¹Centro de Arqueologia da Universidade de Lisboa (UNIARQ), Faculdade de Letras, Universidade de Lisboa, 1600-214 Lisboa, Portugal. ⁴²Centre National de la Recherche Scientifique, University of Lille, Lille, France. ⁴³Department of Anthropology, University of California, Santa Cruz, 1156 High St, Santa Cruz, CA 95064, USA. ⁴⁴Department of Philosophy, Institute of Prehistoric Archaeology, Friedrich-Alexander-University of Erlangen-Nürnberg, 91054 Erlangen, Germany. ⁴⁵Department of Archaeology, Sir Marcus Fernando Mawatha, Colombo 07, Sri Lanka. ⁴⁶Austrian Academy of Sciences, Austrian Archaeological Institute, Hollandstraße 11-13, 1020 Vienna, Austria. ⁴⁷Consell Insular d'Eivissa i Formentera, Avenida de España 49, 07800 Eivissa, Illes Balears, Spain. ⁴⁸Department of Archaeology, Institute of History and Archaeology, University of Tartu, 2 Jakobi St, 51005 Tartu, Estonia. ⁴⁹Secció de Prehistòria i Arqueologia, University of Barcelona, Barcelona, Spain. ⁵⁰Department of Archaeology, Durham University, Durham, UK. ⁵¹Archaeology of Social Dynamics, IMF-CSIC, Barcelona 08001, Spain. ⁵²Cultural Heritage Agency of the Netherlands, Smallepad 5, 3811 MG Amersfoort, The Netherlands. ⁵³Royal Belgian Institute of Natural Sciences, Vautierstraat 29, 1000 Brussels, Belgium. ⁵⁴Laboratory of Biodiversity and Evolutionary Genomics, Katholieke Universiteit Leuven, 3000 Leuven, Belgium. ⁵⁵Department of Archaeology, University of Reading, Berkshire RG6 6AB, UK. ⁵⁶ArchaeoBone, Blekenweg 61, 9753 JN Haren, The Netherlands. ⁵⁷Department of Archaeology, University of Sydney, Sydney, NSW 2006, Australia. ⁵⁸Department of Archaeology, University of Aberdeen, Aberdeen AB24 3UF, UK. ⁵⁹Department of Archaeology, Simon Fraser University, Burnaby, BC V5 1S6, Canada. ⁶⁰Institute of Clinical Molecular Biology, Kiel University, Kiel 24105, Germany. ⁶¹These authors contributed equally: He Yu, Alexandra Jamieson. ✉email: krause@eva.mpg.de; greger.larson@arch.ox.ac.uk; david.orton@york.ac.uk